Temperature analysis of dark current in *pin*-photodiodes based on $In_{0.83}Ga_{0.17}As$/InP epitaxial heterostructures with metamorphic buffer layers

© E.I. Vasilkova[1], O.V. Barantsev[1], A.I. Baranov[1], E.V. Pirogov[1], K.O. Voropaev[2], A.A. Vasiliev[2], L.Ya. Karachinsky[1,3], I.I. Novikov[1,3], M.S. Sobolev[1]

[1] Alferov University,
194021 St. Petersburg, Russia
[2] JSC „OKB-Planeta“,
173004 Veliky Novgorod, Russia
[3] ITMO University,
197101 St. Petersburg, Russia
E-mail: elenvasilkov@gmail.com

Received April 19, 2024
Revised October 10, 2024
Accepted October 10, 2024

Crystals of $2.2-2.6\,\mu$m sensitive *pin*-photodiodes were fabricated by lift-off photolithography using InAlAs/$In_{0.83}Ga_{0.17}As$/InP heterostructures, grown by molecular beam epitaxy. A design feature of the proposed heterostructures is the inclusion of metamorphic InAlAs buffer layers for subsequent low-stress growth of the $In_{0.83}Ga_{0.17}As$ active region. A profile of charge carrier distribution over the structure was obtained employing electrochemical capacitance-voltage characteristic, and the carrier concentration of $2 \cdot 10^{16}\,cm^{-3}$ in the $In_{0.83}Ga_{0.17}As$ active layer was determined. Dark current-voltage characteristics of pin-photodiode chips from the same wafer with typical ($\sim 2\,mA/cm^2$ at $-10\,mV$) and excessive ($\sim 3\,mA/cm^2$ at $-10\,mV$) values of dark currents were studied in the temperature range of $80-300\,K$. Connection of the dark current mechanisms associated with threading dislocations in the photodiode active region with increased dark current densities was demonstrated in the reverse bias voltage range of $0.3-1\,V$. With a small applied bias of $-10\,mV$, the dominant contribution of trap-assisted tunneling and surface recombination at temperatures of $180-240\,K$ and generation-recombination of charge carriers in the space-charge region at $260-300\,K$ to the overall dark current was found in both photodiode chip samples.

Keywords: SWIR photodetectors, dark currents, metamorphic heterostructures, current-voltage characteristic, electrochemical capacitance-voltage profiling.

DOI: 10.61011/SC.2024.07.59540.6329H

1. Introduction

The near-infrared and short-wave infrared photodetectors based on InGaAs/InP heterostructures have many applications in the night visions devices, gas and organic substance spectroscopy devices and etc. [1,2]. The principle of detection is the absorption of radiation from a source by active InGaAs layers and its subsequent conversion into a drift electric current or photocurrent. The long-wavelength limit of the spectral sensitivity range of such photodetectors currently reaches $2.6\,\mu$m due to the use of InGaAs solid solutions with indium content of $\sim 82-83\%$. However, $In_{0.83}Ga_{0.17}As$ and InP materials demonstrate a quite substantial lattice mismatch which is $\sim 2\%$. The lattice mismatch at the epitaxial growth leads to accumulation of elastic stresses which relax through formation of dislocations. Dislocations are structural defects of a crystal, and their presence in the working area of active optoelectronics devices in high concentrations is highly undesirable. In particular, emergence of dislocations in the active area of the photodetector results in a significant increase of dark currents, which, in its turn, adversely affects the detection ability of the device.

Therefore, to provide the lattice match for active layers $In_{0.83}Ga_{0.17}As$ and InP substrate the metamorphic buffer layers are integrated in the photodetector design: these are the semiconductor layers featuring a variable composition in epitaxial growth orientation and used as intermediate layers between the substrate and the active layers. Heterostructures with metamorphic buffer layers are needed when creating a number of devices in order to achieve a low density of defects in the crystalline structure. The buffer layers are generally designed quite massive, about $1-2\,\mu$m thick, depending on type of the structure and purpose of terminal device. Gradual change of composition across the entire buffer thickness provides a smooth transition from a lattice constant of the used substrate to the lattice constant of active area material. At that, such buffer layers may inhibit the emergence of dislocations into the active area, providing their folding.

High quality metamorphic heterostructures, namely $In_{0.83}Ga_{0.17}As$ photodetectors with metamorphic buffer layers may be obtained by method of molecular-beam

epitaxy (MBE) [2–6]. MBE method aimed at growth of semiconductor heterostructures makes it possible to vary the composition of buffer layers with high accuracy and implement complex composition gradient profiles. Such structures with metamorphic buffer layers are characterized by a high degree of relaxation of elastic stresses and a low density of dislocations in the active layer.

Despite a slew of papers on the study of buffer layers for transition from InP substrate to $In_xGa_{1-x}As$ layers with $x > 0.53$ [2,6–9], the photodetectors based on metamorphic heterostructures $In_xGa_{1-x}As/InP$ are characterized by excess dark currents compared to the photodetectors on a lattice-matched pair $In_{0.53}Ga_{0.47}As/InP$. Thus, the density of the dark current of metamorphic InGaAs/InP single-element photodiodes without cooling makes $\sim 0.1-0.5\,mA/cm^2$ at voltage of $-10\,mV$ [10–12], which is by several orders of magnitude higher than the density of the dark current of the lattice-matched InGaAs/InP photodiodes that is about several nA/cm^2 at a room temperature [13].

However, in the spectral range of $2.2-2.6\,\mu m$ the InGaAs/InP-photodetectors outpace the antimonide-based devices [14], including superlattices of II type (T2SL) [15], in terms of dark currents, as well as the CdHgTe technology in terms of cost and manufacturing process simplicity. Thus, major technical and technological benefits of $In_xGa_{1-x}As/InP$ photodetectors in a wide short-wave range of $2.2-2.6\,\mu m$ are the low cost, relatively low dark currents and, hence, high detecting capabilities.

We have demonstrated earlier the crystals of *pin*-photodiodes based on metamorphic $In_{0.83}Ga_{0.17}As/InP$ heterostructures with buffer layers of InAlAs, where we managed to register the photo-response at $2.5\,\mu m$ emission in normal conditions [9]. Typical density of dark current of these photodiodes with reverse bias voltage of $-10\,mV$ was $\sim 1.9\,mA/cm^2$. However, further studies showed that the wafers contained photodiodes crystals with increased values of dark currents $\sim 3\,mA/cm^2$ $(-10\,mV)$, which, most probably, is associated with emergence of a large number of dislocations in the active area of these elements. Thus, this paper is aimed at determining the contribution of leakage currents through dislocations in reverse dark currents of photodiodes with typical and excessive values of dark currents. For this purpose, the temperature dependencies of reverse branches of the photodiodes current-voltage curves in the range of voltages up to $-1\,V$ were obtained and analyzed.

2. Experimental samples

To perform this study we used the crystals of short-wave infrared *pin*-photodiodes based on semiconductor $InAlAs/In_{0.83}Ga_{0.17}As/InP$ heterostructures described in paper [9]. The epitaxial growth of the heterostructures samples was provided on two doped substrates n^+-InP (100) of „epi-ready“ quality with the use of Riber MBE49 system. The area of metamorphic buffer layer contained $In_yAl_{1-y}As$ layers with total thickness of $2\,\mu m$ with a linear indium content gradient from 52 to 86% and auxiliary thin inserts, each of which comprised three periodic repetitions of InAs (4 Å)/InAlAs (10 Å) superlattices. At the end of the gradient layer growth a peak annealing at a temperature of 630°C was performed followed by further substrate holder temperature decline to 50°C. In details the conditions of epitaxial growth of these metamorphic buffer layers are outlined in paper [6]. To form *pin*-photodiodes crystals the buffer layers were doped with silicon (n^+), and contact layers InAlAs/InGaAs with total thickness of $0.62\,\mu m$ were doped with beryllium (p^+). Active area $In_{0.83}Ga_{0.17}As$ with a thickness of $1.5\,\mu m$ was also uniformly doped with silicon in small concentrations of the *n*-type impurity $\sim 5 \cdot 10^{15}\,cm^{-3}$ (n) while performing the functions of *i*-region in the heterostructure of *pin*-photodiode.

Using the lift-off photolithography on a double masking photoresist the *p*- and *n*-type, ohmic contacts based on a low-resistance Ti/Pt/Au system of metals, as well as anode and cathode V/Au metallization contact areas, were formed

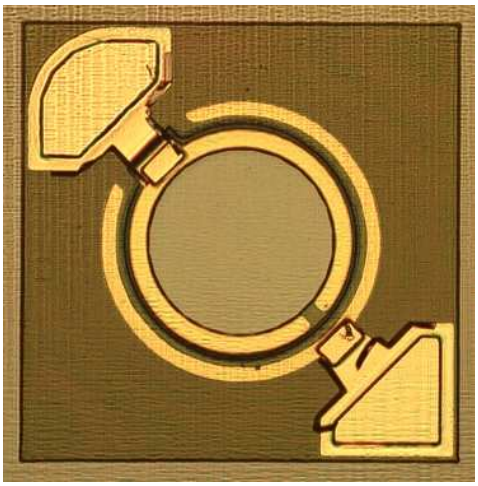

Figure 1. Photo of *pin*-photodiode crystal.

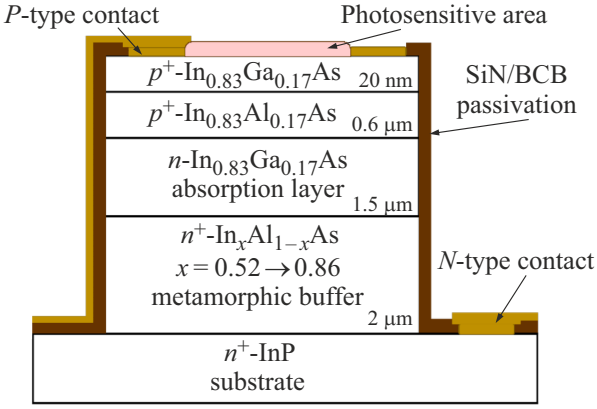

Figure 2. Schematic representation of *pin*-photodiode cross-section.

for the MPE fabricated heterostructure. The wafer surface was passivated by Plasma Enhanced Chemical Vapor Deposition (PECVD) of the silicon nitride (SiN) layer 276 nm thick followed by application of benzocyclobutene (BCB) layer 4 μm thick. The photo-sensitive area of obtained *pin*-photodiode crystals was $\sim 140\,\mu$m in diameter. The photo of a crystal of *pin*-photodiode is shown in Figure 1, and the cross-section of layers structure is schematically shown in — Figure 2.

3. Results and discussion

The experimental samples have been tentatively examined using standard and electrochemical capacitance-voltage (ECV) profiling techniques. The earlier calculated shunting capacitance of *pin*-photodiodes crystals with minimal values of dark currents turned out to be equal 14 pF [9]. ECV-profile of distribution of the main charge carriers across the heterostructure obtained using electrochemical profilometer ECV Pro (Nanometrics, USA) is given in Figure 3. The carriers distribution profile is specific for $p-i-n$-transition, where as i-area the layer n-$In_{0.83}Ga_{0.17}As$ lightly doped with silicone is used. The thicknesses of areas for each type of carriers correspond to the thicknesses of contact, active and metamorphic buffer layers provided in the growth program. At depths, relating to the active area, there's an area of electrons concentration fluctuations, and in the buffer layers — drastic spikes are observed. These artifacts are suggested to be associated with the manifestation of the shunting properties of emerging dislocations. However, we could assess the concentration of charge carriers in i-area, it was equal $\sim 2.5 \cdot 10^{16}\,\mathrm{cm}^{-3}$. Concentrations of the charge carriers of the respective sign in p^+ and n^+ areas were $\sim (1-2) \cdot 10^{18}\,\mathrm{cm}^{-3}$.

The discrepancy between the experimental concentration value and the one set for MBE growth is caused by insufficient detail of the calibration curve of the silicon atoms flow in the region of low heating temperatures of the effusion source, which is why the temperature of the silicon source at the time of synthesis of the heterostructure was set too high. Yet, the obtained level of doping of the high-resistance layer allows to form a structure with a drastic p^+-n-transition suitable for manufacture of a photodiode. Thus, with further analysis of the experimental current-voltage curves the actual doping level for $In_{0.83}Ga_{0.17}As$ layer was considered equal $\sim 2.5 \cdot 10^{16}\,\mathrm{cm}^{-3}$, as obtained in the experiment.

The current-voltage curves of *pin*-photodiode crystals have been studied earlier at room temperature and applied bias voltages from -1 to 0.25 V. The corresponding curves of several samples measured at room temperature, were demonstrated and described in paper [9]. With the bias voltage of -1 V the dark currents of the reverse branch were in average $\sim 10\,\mu$A, which corresponds to the current density of $0.065\,\mathrm{A/cm}^2$, and at a small bias

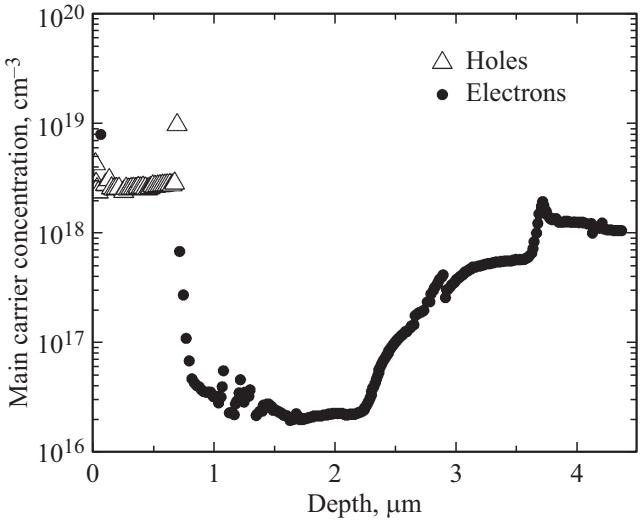

Figure 3. Charge carriers concentration distributed across the heterostructure reached by electrochemical capacitance-voltage (ECV) profiling technique.

voltage of -10 mV the reverse current was equal ~ 300 nA, or $1.9\,\mathrm{mA/cm}^2$. The shunting resistance R_0, calculated complying with a general approach at bias voltage of 10 mV [16] for these samples was ~ 25 kOhm, and their production was $R_0A \sim 4\,\mathrm{Ohm} \cdot \mathrm{cm}^2$. Samples with dark high currents were characterized by the following parameters: dark current $\sim 69\,\mu$A or $0.45\,\mathrm{A/cm}^2$ at voltage of -1 V, ~ 470 nA or $3\,\mathrm{mA/cm}^2$ at voltage of -10 mV, resistance R_0 ~ 18 kOhm and $R_0A \sim 3\,\mathrm{Ohm} \cdot \mathrm{cm}^2$.

To study the mechanisms of the formation of reverse dark currents, the samples current-voltage curves were obtained in a wide temperature range from 80 to 300 K, with an increment of 20 K. The values of dark currents were obtained at bias voltage of -1 up to 0.1 V per every 10 mV. The samples were cooled using Janis VPF-100, cryostat and the current-voltage curve were obtained by measurements with Keithley 2400 measuring source. At this stage of the study the sample PD-1 of *pin*-photodiode crystal that demonstrated minimal dark current and the sample PD-2 that had an excessive dark current were compared. The corresponding families of the current-voltage curves of samples are given in Figure 4. The figures are made in semi-logarithmic scale, at that the reverse branches of the dark currents are depicted in the upper semi-plane.

The dark currents flowing in photodiodes are an important characteristic that determines the intensity of radiation that the device is able to detect and distinguish at the noise level. To obtain a device with better sensitivity we need to understand the nature of the dark currents formation in the heterostructure of *pin*-photodiode. Total dark current is composed of several components, namely: a) thermal diffusion current of secondary charge carriers in neutral p- and n-areas, b) charge carriers generation-recombination current in the depletion band through Shockley–Read–Hall centers in the area of the bulk charge c) tunneling currents

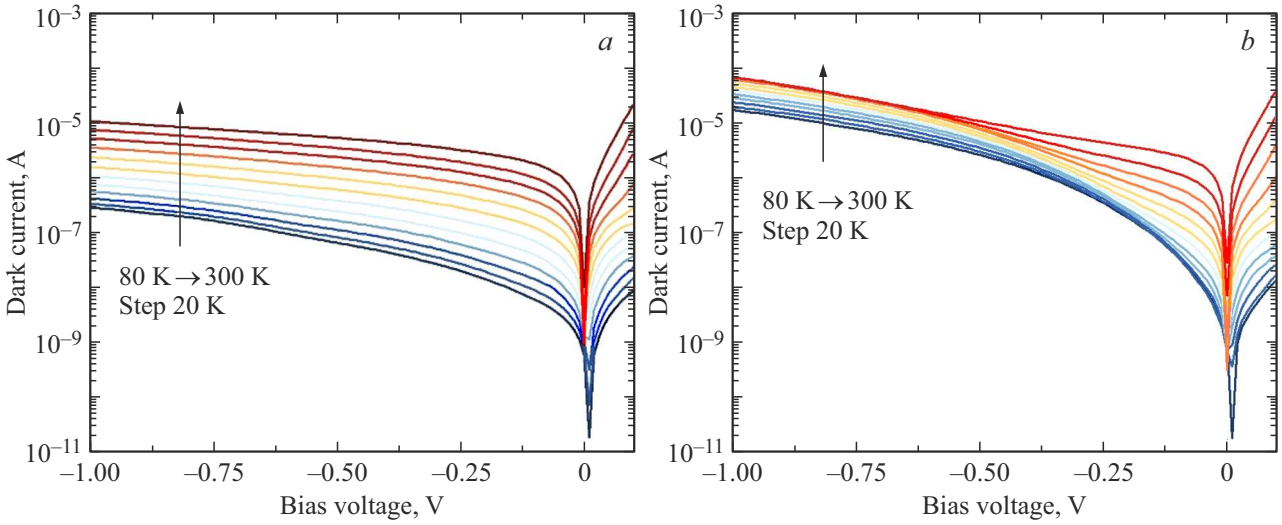

Figure 4. Current-voltage curves of samples PD-1 (a) and PD-2 (b) of pin-photodiodes crystals obtained at temperatures 80–300 K. (A color version of the figure is provided in the online version of the paper.)

through traps in the band gap, d) inter-band tunneling current, e) surface, shunting leakage currents [8,10,17]. The sources of states in the band gap amplifying the effects of Shockley–Read–Hall generation-recombination mechanisms and tunneling through the traps may be caused by the emerging dislocations.

The photodiode currents are known to have different dependence from the applied voltage and temperature. It is known that in ideal p–n-transition the diffusion component provides major contribution to the direct orientation of current flow at positive bias, and in case of negative bias $\gtrsim 2kT/e$ (where k — Boltzmann constant, T — temperature, e — electron charge) it becomes small and is practically independent of voltage [18]. The generation-recombination current has a root cause dependence of the applied bias voltage and may introduce sufficient contribution to the dark current flowing in both directions, especially at low temperatures [19–21]. Tunneling currents also have a pronounced dependence on the applied voltage, while a smaller bias shall be applied to activate tunneling through deep traps compared to the inter-band tunneling under other identical conditions [20].

Figure 4, a illustrates that with the sample temperature decline over the entire region of the studied voltages the expected drop in the dark currents by about ~ 2 orders of magnitude is observed. At the same time, at all the studied temperatures, there is a drastic increase of current in the reverse voltage range from 0 to 0.1 V with further access to the current saturation region, however, the flat saturation area of the current-voltage curve is more pronounced at temperatures close to room temperature. Thus, we may suggest that at reverse voltages from 0.1 to 1 V in the PD-1 sample, the diffusion component of the dark current prevails at higher temperatures, and in the region of nitrogen temperatures, the contribution of generation-recombination and tunneling mechanisms depending on the magnitude of the displacement is observed.

In Figure 4, b, on the contrary, at voltages from -1 to -0.3 V the dark currents vary insignificantly and their values stay within the range of microamperes, even at a temperature of 80 K. At that, in the entire temperature range the reverse current continues to grow with the growth of reverse voltage up to 1 V. Thus, in case of PD-2 sample the diffusion mechanism is not predominant in generation of the dark current at reverse bias from -1 to -0.3 V, and excessive influence of the generation-recombination and tunneling currents through the traps becomes evident. This fact proves the suggestion that dislocations may intrude into the active area of PD-2 sample.

At low voltages, the dependence of the reverse dark current on temperature is generally exponential: $I_T \sim \exp(-E_a/kT)$ [18]. In this ratio k — Boltzmann constant, T — temperature, E_a — activation energy. At that, various values of E_a correspond to different mechanisms of dark currents occurrence mechanisms. The diffusion mechanism is provided by the activation energy, approximately equal to the width of the band gap of active region E_g (~ 0.48) eV, and the regeneration-recombination mechanism is provided by $E_g/2$ (~ 0.24 eV) in the recombination model through the Shockley–Read–Hall centers (levels of defects in the depletion region) [18]. The activation energy of the charge carriers surface recombination is described as $\leq E_g/4$ (~ 0.12 eV) [7,10], however, the mechanism of surface leakages in general is poorly studied and requires additional review [20]. In addition, low activation energies are usually correlated with the predominance of tunneling mechanisms. Thus, according to [22], the tunneling through traps may have activation energies in the range from 0.1 eV to $E_g/2$, also being defined by some researchers as equal to $E_g/4$ [10]. Regular decrease in the band gap width with

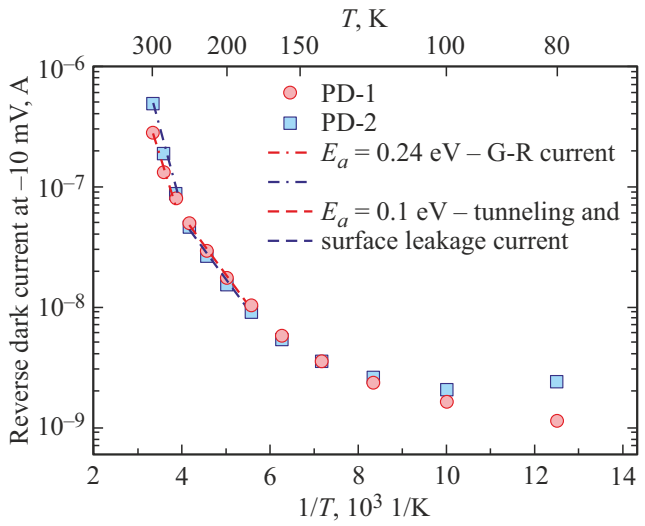

Figure 5. Approximation of experimental temperature dependence of reverse dark currents of the photodiodes crystal samples at -10 mV for various values of E_a.

heating [23] in InGaAs results in characteristic activation energies of zone−zone < 0.1 eV tunneling [22].

To define the predominant mechanism of dark currents in the studied crystals of *pin*-photodiodes at small bias voltages the curves of the dark current intensity versus value reciprocal of temperature, in the given range 80−300 were plotted. Exterior potentials difference was equal -10 mV. Then, this dependence was approximated by several functions $F(T) = C\exp(-E_a/kT)$, where C — temperature-independent constant. Values E_a were taken equal E_g, $E_g/2$, $E_g/4$ and 0.1 eV consistent with the dark currents occurrence mechanisms described above.

As a result, for both samples the temperature areas were delineated where different dark currents formation mechanisms prevailed (Figure 5). It should be noted that despite significant difference of the current-voltage curves between PD-1 and PD-2 samples (Figure 4), the dependencies analyzed in Figure 5 are practically identical. The discrepancies between the experimental points are observed at boundary values of the studied temperatures i. e. at room temperatures (280−300 K), that has been mentioned earlier, and at liquid nitrogen temperature (80 K). At bias voltage of -10 mV in 260−300 K area the major contribution to the dark current of PD-1 and PD-2 samples is provided by the regeneration-recombination mechanism. 180−240 K temperature area is optimally approximated by the function with activation energy equal ~ 0.1 eV, which allows us suggesting the existence of surface leaks and tunneling through the deep levels. At lower temperatures the current intensity varies slightly with the temperature change which indicates of activation energies of ~ 0.01 eV. For this area we may also speak of the surface leaks and tunneling mechanisms contribution, including zone−zone tunneling due to small assumed activation energies $E_a \ll E_g$.

Thus, both, PD-1 sample, with minimal dark current and PD-2 sample with high dark current at small bias voltages of -10 mV in a wide temperature range 180−300 K may have components of the dark current associated with high density of the emerging dislocations. One of the ways the dislocations density may be reduced in heterostructures of *pin*-photodiodes, and, hence, accompanied by the reduced generation-recombination and tunnel components of the dark current, is using the inserts of $In_{0.83}Ga_{0.17}As/In_{0.83}Al_{0.17}As$ „digital-graded superlattices“ at the buffer layer/active area and active area/contact layer interfaces [2]. Moreover, it is required to additionally study the processes of surface recombination of the charge carriers, as well as the contribution of surface leaks into formation of dark current in one or another temperature ranges.

4. Conclusion

This paper outlines the studies of the current-voltage curves of *pin*-photodiodes crystals in 2.2−2.6 μm spectral range with various dark currents fabricated from In(Al)GaAs/InP heterostructures with $In_yAl_{1y}As$ ($y = 0.52$−0.86) metamorphic buffer layers obtained by MBE. By using the electrochemical capacitance-voltage (ECV) profiling it was demonstrated that distribution of the major charge carriers in the fabricated heterostructures corresponds to $p-i-n$-transition with the carriers concentration in i-area of $2.5 \cdot 10^{16}$ cm^{-3}. From the studies of the current-voltage curves of photodiodes crystals it was found that in the range of reverse voltages of 0.1−1 V the sample PD-1 featuring minimal dark currents mainly has diffusion dark current, while PD-2 sample with excess dark currents has a contribution of the generation-recombination and trap tunneling currents dependent on the dislocations density. At that, in the area of -10 mV small voltages both samples have identical types of dark current versus temperature curves. In these conditions the dark currents are mainly generated due to the mechanisms of the charge carriers generation-recombination in the bulk charge area (260−300 K) and tunneling through traps and surface recombination of carriers (180−240 K).

Funding

The study was supported financially by the Russian Scientific Fund within the scientific project No. 22-79-00146 and by the Ministry of Science and Higher Education of the Russian Federation within the scope of the state assignment No. FSRM-2022-0002.

Conflict of interest

The authors declare that they have no conflict of interest.

References

[1] I.D. Burlakov, L.Ya. Grinchenko, A.I. Dirochka, N.B. Zaletaev. UPF, **2** (2), 131 (2014). (in Russian).
[2] X. Chen, Y. Gu, Y. Zhang. *Epitaxy and device properties of InGaAs photodetectors with relatively high lattice mismatch, in Epitaxy* (IntechOpen, Rijeka, 2018).
[3] L.Y. Karachinsky, T. Kettler, I.I. Novikov, Y.M. Shernyakov, N.Y. Gordeev, M.V. Maximov, N.V. Kryzhanovskaya, A.E. Zhukov, E.S. Semenova, A.P. Vasil'ev. Semicond. Sci. Technol., **21** (5), 691 (2006).
[4] A.Yu. Egorov, L.Ya. Karachinsky, I.I. Novikov, A.V. Babichev, T.N. Berezovskaya, V.N. Nevedomskiy. Semiconductors, **49** (10), 1388 (2015).
[5] A.Yu. Egorov, L.Ya. Karachinsky, I.I. Novikov, A.V. Babichev, V.N. Nevedomskiy, V.E. Bugrov. Semiconductors, **50** (5), 612 (2016).
[6] E.I. Vasilkova, E.V. Pirogov, M.S. Sobolev, E.V. Ubyivovk, A.M. Miserov, P.V. Seredin. Kondensirovannye sredy i mezhfaznye granitsy, **25** (1), 20 (2023).
[7] X.Y. Chen, Y. Gu, Y.G. Zhang, Y.J. Ma, B. Du, H.Y. Shi, W.Y. Ji, Y. Zhu. Infr. Phys. Technol., **89**, 381 (2018).
[8] X. Ji, B. Liu, H. Tang, X. Yang, X. Li, H. Gong, B. Shen, P. Han, F. Yan. AIP Adv., **4** (8), 087135 (2014).
[9] E.I. Vasilkova, E.V. Pirogov, K.Yu. Shubina, K.O. Voropaev, A.A. Vasiliev, L.Ya. Karachinsky, I.I. Novikov, O.V. Barantsev, M.S. Sobolev. Kondensirovannye sredy i mezhfaznye granitsy, **26** (3), 417 (2024). (in Russian).
[10] Y. Liu, Y. Ma, X. Li, J. Fang. IEEE J. Quant. Electron., **56** (2), 1 (2020).
[11] Z. Jiao, T. Guo, G. Zhou, Y. Gu, B. Liu, Y. Yu, C. Yu, Y. Ma, T. Li, X. Li. Electronics, **13**, 1339 (2024).
[12] L. Wan, X. Shao, Y. Ma, S. Deng, Y. Liu, J. Cheng, Y. Gu, T. Li, X. Li. Infr. Phys. Technol., **109**, 103389 (2020).
[13] C.-C. Huang, C.-L. Ho, M.-C. Wu. IEEE Electron Dev. Lett., **36** (10), 1066 (2015).
[14] I. Shafir, N. Snapi, D. Cohen-Elias, A. Glozman, O. Klin, E. Weiss, O. Westreich, N. Sicron, M. Katz. Appl. Phys. Lett., **118** (6), 063503 (2021).
[15] Y. Liang, W. Zhou, X. Zhang, F. Chang, N. Li, Y. Shan, Y. Zhang, F. Ye, C. Li, X. Su, C. Yang, H. Hao, G. Wang, D. Jiang, D. Wu, H. Ni, Y. Xu, Z. Niu, Y. Zheng, Y. Shi. Appl. Phys. Lett., **125** (14), 141103 (2024).
[16] P.R. Thompson, T.C. Larason. *Method of measuring shunt resistance in photodiodes, in 2001 Measurement Sci. Conf.* (2001).
[17] N.I. Yakovleva, K.O. Boltar. Prikl. Fiz., **3**, 66 (2015). (in Russian).
[18] S.M. Sze. *Physics of semiconductor devices* (John Wiley & Sons, 1969).
[19] N.I. Yakovleva. UPF, **6** (3), 231 (2018). (in Russian).
[20] A.V. Sorochkin, V.S. Varavin, A.V. Predein, I.V. Sabinina, M.V. Yakushev. FTP, **46** (4), 551 (2012). (in Russian).
[21] K. Taguchi. *P–I–N Photodiodes, in WDM Technologies: Active Optical Components* (Elsevier, 2002).
[22] Q. Smets, D. Verreck, A.S. Verhulst, R. Rooyackers, C. Merckling, M. Van De Put, E. Simoen, W. Vandervorst, N. Collaert, V.Y. Thean, B. Sorée, G. Groeseneken, M.M. Heyns. J. Appl. Phys., **115** (18), 184503 (2014).
[23] Y.P. Varshni. Physica, **34** (1), 149 (1967).

Translated by T.Zorina